

# Assessment of Aerodynamic Challenges of a Variable-Speed Power Turbine for Large Civil Tilt-Rotor Application

*Gerard E. Welch*  
*Glenn Research Center, Cleveland, Ohio*

## NASA STI Program . . . in Profile

Since its founding, NASA has been dedicated to the advancement of aeronautics and space science. The NASA Scientific and Technical Information (STI) program plays a key part in helping NASA maintain this important role.

The NASA STI Program operates under the auspices of the Agency Chief Information Officer. It collects, organizes, provides for archiving, and disseminates NASA's STI. The NASA STI program provides access to the NASA Aeronautics and Space Database and its public interface, the NASA Technical Reports Server, thus providing one of the largest collections of aeronautical and space science STI in the world. Results are published in both non-NASA channels and by NASA in the NASA STI Report Series, which includes the following report types:

- **TECHNICAL PUBLICATION.** Reports of completed research or a major significant phase of research that present the results of NASA programs and include extensive data or theoretical analysis. Includes compilations of significant scientific and technical data and information deemed to be of continuing reference value. NASA counterpart of peer-reviewed formal professional papers but has less stringent limitations on manuscript length and extent of graphic presentations.
- **TECHNICAL MEMORANDUM.** Scientific and technical findings that are preliminary or of specialized interest, e.g., quick release reports, working papers, and bibliographies that contain minimal annotation. Does not contain extensive analysis.
- **CONTRACTOR REPORT.** Scientific and technical findings by NASA-sponsored contractors and grantees.

- **CONFERENCE PUBLICATION.** Collected papers from scientific and technical conferences, symposia, seminars, or other meetings sponsored or cosponsored by NASA.
- **SPECIAL PUBLICATION.** Scientific, technical, or historical information from NASA programs, projects, and missions, often concerned with subjects having substantial public interest.
- **TECHNICAL TRANSLATION.** English-language translations of foreign scientific and technical material pertinent to NASA's mission.

Specialized services also include creating custom thesauri, building customized databases, organizing and publishing research results.

For more information about the NASA STI program, see the following:

- Access the NASA STI program home page at <http://www.sti.nasa.gov>
- E-mail your question via the Internet to [help@sti.nasa.gov](mailto:help@sti.nasa.gov)
- Fax your question to the NASA STI Help Desk at 443-757-5803
- Telephone the NASA STI Help Desk at 443-757-5802
- Write to:  
NASA Center for AeroSpace Information (CASI)  
7115 Standard Drive  
Hanover, MD 21076-1320



# Assessment of Aerodynamic Challenges of a Variable-Speed Power Turbine for Large Civil Tilt-Rotor Application

*Gerard E. Welch*  
*Glenn Research Center, Cleveland, Ohio*

Prepared for the  
66th Annual Forum and Technology Display (AHS Forum 66)  
sponsored by the American Helicopter Society  
Phoenix, Arizona, May 11–13, 2010

National Aeronautics and  
Space Administration

Glenn Research Center  
Cleveland, Ohio 44135

## Acknowledgments

The author is indebted to Mr. Robert J. Boyle (former NASA Glenn Research Center (GRC) Distinguished Research Associate) for innumerable conversations related to variable-speed power turbine, to Mr. Christopher A. Snyder (NASA GRC/RTM) for continued efforts in setting and refining the Large Civil Tilt-Rotor (LCTR) power-turbine requirements, and to Dr. Rodrick V. Chima for assistance with his Reynolds-Averaged Navier-Stokes (RANS) tools. The author is indebted to Dr. John P. Clark, Air Force Research Laboratory (AFRL) for sharing his insights concerning computational modeling of transitional LPT flows, for providing the L1-series blade sections, and for generously installing the AFRL Turbine Design and Analysis System (TDAAS) at NASA.

This report contains preliminary findings,  
subject to revision as analysis proceeds.

*Level of Review:* This material has been technically reviewed by technical management.

Available from

NASA Center for Aerospace Information  
7115 Standard Drive  
Hanover, MD 21076-1320

National Technical Information Service  
5301 Shawnee Road  
Alexandria, VA 22312

Available electronically at <http://gltrs.grc.nasa.gov>

# Assessment of Aerodynamic Challenges of a Variable-Speed Power Turbine for Large Civil Tilt-Rotor Application

Gerard E. Welch  
National Aeronautics and Space Administration  
Glenn Research Center  
Cleveland, Ohio 44135

## Abstract

The main rotors of the NASA Large Civil Tilt-Rotor notional vehicle operate over a wide speed-range (100% at take-off to 54% at cruise). The variable-speed power turbine, when coupled to a fixed-gear-ratio transmission, offers one approach to accomplish this speed variation. The key aerodynamic challenges of the variable-speed power turbine are related to high work factors at cruise, where the power turbine operates at 54% of take-off speed, wide incidence variations into the vane, blade, and exit-guide-vane rows associated with the power-turbine speed change, and the impact of low aft-stage Reynolds number (transitional flow) at 28 kft cruise. Meanline and 2-D Reynolds-Averaged Navier-Stokes analyses are used to characterize the variable-speed power-turbine aerodynamic challenges and to outline a conceptual design approach that accounts for multi-point operation. Identified technical challenges associated with the aerodynamics of high work factor, incidence-tolerant blading, and low Reynolds numbers pose research needs outlined in the paper.

## Nomenclature

$AN^2$	product of annulus area and rpm-squared
$AR$	$(r_t - r_h)/c_x$ , blade aspect ratio
$c_x$	axial chord
$f$	$N/N_{100\%}$ , speed ratio factor
$h_0, h$	total and static specific enthalpy
$i, i_s$	incidence, incidence at suction-side stall
$\dot{m}$	mass flow rate
$M, M_r$	absolute and relative Mach numbers
$N$	power-turbine shaft speed, rpm
$N_{stg}$	number of turbine stages (stator/rotor)
$p_0, p$	total and static pressure
$r_h, r_t$	hub and tip radii
$R_{stg}$	$(h_1 - h_2)/(h_{0,0} - h_{0,2})$ , stage enthalpy reaction
$Re_{cx}$	Reynolds number based on axial chord
$s$	blade pitch
$\underline{u}$	$(u_x, u_\theta)$ , absolute velocity
$U$	rotor speed at pitchline
$\underline{w}$	$(u_x, u_\theta - U)$ , relative velocity
$\dot{W}$	shaft power
$V_j$	Speed of isentropic expansion through $PR_{T-T}$
$Z$	$\frac{s}{c_x} \frac{\rho u_x (u_{0,1} - u_{0,2})}{p_{0,r,1} - p_2}$ , Zweifel loading parameter
$\alpha, \beta$	absolute and relative flow angles

$\eta_{stg}$	stage efficiency (total-to-total)
$\rho$	density
$\mu_t, \mu_l$	turbulent, laminar viscosity
$\psi$	$\Delta h_0/U^2$ , work factor
$\phi$	$u_x/U$ , flow coefficient

## Subscripts

$c$	corrected condition
$des$	design point
$0, 1, 2$	Stations: nozzle inlet, rotor inlet, rotor exit
$4.5$	power turbine inlet
$n$	nozzle (vane)
$r$	rotor (blade), or relative condition
$opt$	optimum

## Introduction

A principal goal of the Subsonic Rotary Wing project of the NASA Fundamental Aeronautics program is to enhance the throughput capacity of airports by increased utilization of civil rotorcraft (see Johnson *et al.* (Ref. 1) and Wilkerson and Smith (Ref. 2)). The technical objectives of this project require development and maturation of technologies to enable a large vertical takeoff and landing (VTOL) transport, capable of Mach 0.5 forward cruise at 28 kft, with a range greater than 1000 nm. Vehicle systems studies of large civil rotorcraft concepts have resulted in mission refinement and the definition of a notional Large Civil Tilt-Rotor (LCTR) vehicle that helps define the technical challenges and research requirements (Johnson *et al.* (Ref. 1) and Acree *et al.* (Ref. 3)). Fuel efficiency is of prime importance and must be maximized by balancing fuel-burn penalties associated with variable-speed engine/drive-train capability with gains achieved by slowing the main rotor speed substantially (to 54% of take-off speed, cf. Acree (Ref. 4)) as required to maintain high propeller efficiencies at cruise flight speeds.

The required main-rotor speed variation from 100% at take-off (e.g., 650 ft/s tip speed) to near 54% (350 ft/s) at cruise can be achieved by use of a multi-speed transmission driven by a power turbine (PT) operating with minimal required speed change. Alternatively, the speed variation can be achieved by using a variable-speed power turbine (VSPT) driving a rotorcraft transmission with fixed gear ratio. The increase in fuel burn from the added weight of a multi-speed transmission can be traded against the capabilities and penalties of a VSPT;

Prop/rotor and PT design point efficiency versus percent Npt MDHC TW rotor, 3 stage fixed geometry PT, Max cruise at M = 0.7

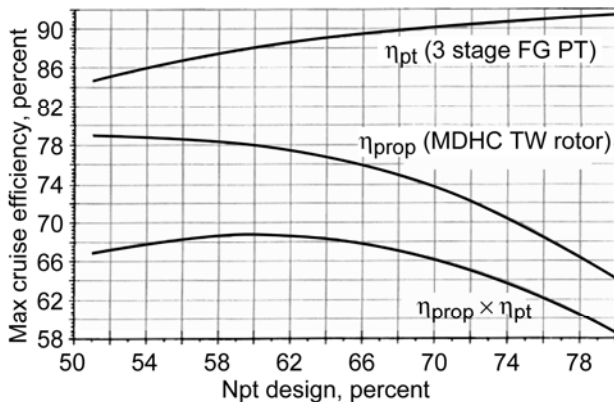


Figure 1.—Cruise efficiencies of power turbine, main rotor, and their product as a function of power turbine design speed (reproduced from D’Angelo, Ref. 5).

indeed, a combination of turbine speed change and variable transmission may prove optimal. The work reported here is focused on achieving main-rotor speed variation by power-turbine speed variation alone—*i.e.*, assuming a fixed, single-gear ratio transmission. This speed variation approach is used in the V-22, albeit over a narrower range ( $0.82 < N/N_{100\%} < 1$ , Wilkerson and Smith<sup>2</sup>) than considered in the present study ( $0.54 < N/N_{100\%} < 1$ ).

The results from an earlier tilt-rotor study (Figure 1 from D’Angelo (Ref. 5)) showed the trade-off between main-rotor prop efficiency and design-point power-turbine efficiency as a function of turbine operating speed. Although the particular Mach 0.7, 15 kft cruise point considered by D’Angelo (Ref. 5) is substantially different from the LCTR cruise conditions considered herein, the following relevant points are illustrated (Fig. 1). The strong increase in propulsive efficiency (*e.g.*, 15 pts.) achieved by slowing the main rotor motivates the variable-speed rotor requirements of the LCTR; however, as the main rotor and power turbine slow, the design-point efficiency of the power-turbine drops strongly (*e.g.*, 5 to 10 pts., see Fig. 1). Consideration of the product of the two efficiencies indicates that there is an optimum cruise speed in terms of fuel burn.

The strong lapse in power-turbine design-point efficiency with decreasing speed can be offset somewhat by designing the power-turbine at, or near, its cruise speed (54% of take-off in this study) so that losses associated with positive incidence are mitigated; even so, as shown in the next section, the high work factors (flow turning) required at the lower PT speeds will inevitably result in lower efficiencies than can be achieved in a turbine optimized for near constant high-speed (100%) operation.

Operation of a power turbine over a wide speed range ( $54\% < N/N_{100\%} < 100\%$ ) represents a strong departure from

traditional, nearly constant, power-turbine speed operation. The wide-speed operation poses formidable aerodynamic and mechanical challenges. The key aerodynamic challenges confronting the VSPT include a high work factor at cruise, a wide incidence variation between cruise and take-off, and low aft-stage Reynolds numbers at cruise altitudes. These challenges are discussed in the next section. A conceptual-design approach for the VSPT is then outlined, and candidate designs that meet the LCTR engine requirements are provided. Findings from preliminary research related to incidence tolerant blading and low-Re flows are reported, with the intent to elucidate research needs. Finally, an overview of a VSPT research effort underway at NASA GRC is provided.

## Aerodynamic Challenges

Relevant engine/VSPT requirements for key flight points of the LCTR mission are provided in Table 1 (Snyder and Thurman (Ref. 6)). The requirements reflect the load demand of the variable-pitch main rotor of the LCTR. The gas generator (LP and HP spools) operates with fixed geometry between sea-level take-off and 28 kft cruise, and the lapse in engine power and flow is associated with altitude changes alone. The fuel-throttle settings at the sea-level and cruise points are essentially constant, and hence, so is the corrected flow through the engine. The engine runs at essentially full power, when corrected for altitude, over the entire mission, although component temperatures at cruise are lower due to altitude-related temperature changes.

Note that the power-turbine enthalpy extraction levels (*i.e.*, specific power,  $\Delta h_0 = \dot{W}/\dot{m} = \Delta(u_\theta U)$ ) at 2 kft take-off (100% speed) and 28 kft cruise (54, 62, 75, and 100% speed) are essentially constant. This leads to strong VSPT aero-performance implications associated with high work factors at the 54%-speed cruise point and large incidence variation on the vanes and blades as the VSPT speed is changed. The low aft-stage Reynolds numbers (transitional flow) additionally burden the power turbine with higher design-point loss levels and reduced incidence-range capability. These challenges are discussed in this section.

## Efficiency at High Work Factors

The mission requirement for near constant enthalpy extraction at take-off and cruise requires that the work factor,  $\psi = \Delta h_0 / U^2$ , at cruise (54% speed) will be approximately 3.5 times higher than at take-off (100% speed). To ensure that take-off work factors are unity or above for weight mitigation, cruise work factors are 3.5 to 4. Attainment of high efficiency blade rows at such high work factors constitutes a key technical challenge and objective for the variable-speed power-turbine aerodynamic design effort. The challenge is evident in the Smith charts of Figure 2, where stage efficiency is plotted as a function of work factor and flow coefficient for a family of low (0.2 to 0.3) reaction turbines. Figure 2(a) was

TABLE 1.—VSPT REQUIREMENTS AT KEY FLIGHT POINTS OF LCTR MISSION (SNYDER AND THURMAN (REF. 6)).

Flight point	Take-off	Cruise	Cruise	Cruise	Cruise
Altitude	2 kft	28 kft	28 kft	28 kft	28 kft
VSPT speed ( $N/N_{100\%}$ )	100%	54%	61.5%	75%	100%
Main-rotor tip-speed	650 ft/s	350 ft/s	400 ft/s	500 ft/s	650 ft/s
Power, SHP	4593	2328	2330	2329	2330
VSPT mass flow rate, $lb_m/s$	22.03	12.22	11.71	11.63	11.55
Specific power (SHP/ $lb_m/s$ )	208.5	190.5	200.2	200.2	201.8
PT inlet temp ( $T_{4.5}$ ), R	2204	1812	1798	1795	1818
PT inlet pres. ( $p_{0.4.5}$ ), psia	58.0	26.76	26.3	26.1	26.6
PT pressure ratio (total-to-total)	4.04	5.34	5.25	5.21	5.30
Corrected flow, $lb_m/s$	11.51	12.54	12.41	12.18	11.95
Corrected speed ( $N_c/N_{c100\%}$ )	102.3	60.8	69.7	85.1	112.7
Aft-stage unit-Re (in. <sup>-1</sup> ) <sup>a</sup>	50,000/in.	30,000/in.	30,000/in.	30,000/in.	30,000/in.

<sup>a</sup>Based on static conditions at last stage rotor exit with  $M_{r,2} = 0.7$ .

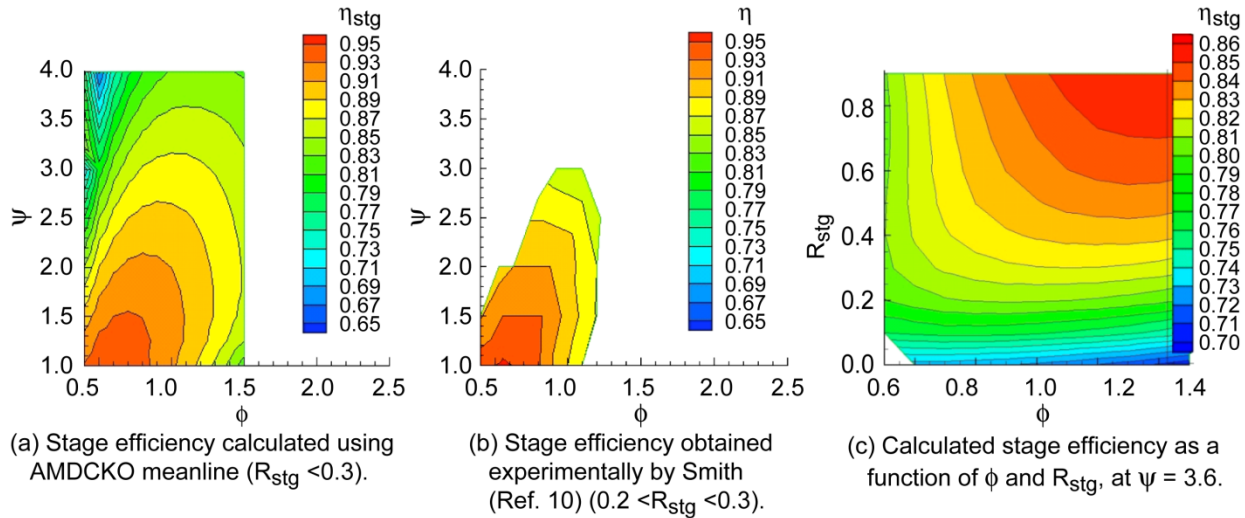


Figure 2.—Calculated and experimental design-point total-to-total stage efficiency as a function of work and flow coefficient and stage reaction, for a family of turbines with averaged stage reaction of 0.25,  $r_h/r_t = 0.7$ ,  $AR = 5$ ,  $Re = 5 \times 10^5$ ,  $M_{r,2} = 0.7$ ,  $Z_r = Z_n = 0.8$ , with zero clearance.

generated using the design-point methodology of Ainley and Mathieson (Ref. 7) with the modifications implemented by Dunham and Came (Ref. 8) and Kacker and Okapuu (Ref. 9), referred to as AMDCKO herein. The calculated efficiencies compare well with the experimental data (Fig. 2(b)) of Smith (Ref. 10) (as reported in Horlock (Ref. 11)). The strong decrease in maximum achievable stage efficiency with increasing work factor is evident in the figure.

Considering Figure 2, the design-point flow coefficient can be selected to optimize efficiency for a given work factor level. Note however that the flow angle variation into embedded blade rows will generally decrease with increasing flow factor; therefore, as work factor is reduced, and the optimum design-point flow coefficient for maximum efficiency decreases, the associated incidence variations into embedded stages (and exit guide vane) would be expected to increase (cf. D'Angelo (Ref. 5)). The influence of stage

reaction and flow coefficient on the stage efficiency of an example turbine with work factor of 3.6 is shown in Figure 2(c).

In Figure 3, turbine design-point stage efficiency (total-to-total) is plotted as a function of average stage work factor for a number of turbine designs. The design-point stage efficiency decreases strongly with work factor. Relative to a PT operating at fixed (high) speed, as in a traditional helicopter engine or in an LCTR variant with a variable-speed transmission, there is a substantial efficiency debit associated with operation at high work factors. Viable VSPT designs must necessarily minimize this debit. The work factor (efficiency debit) can be minimized by adding turbine stages—weight—and by increasing pitchline speeds at cruise (high stress levels at take-off speeds). These options are investigated in the LCTR Power Turbine Conceptual Design section of this paper.

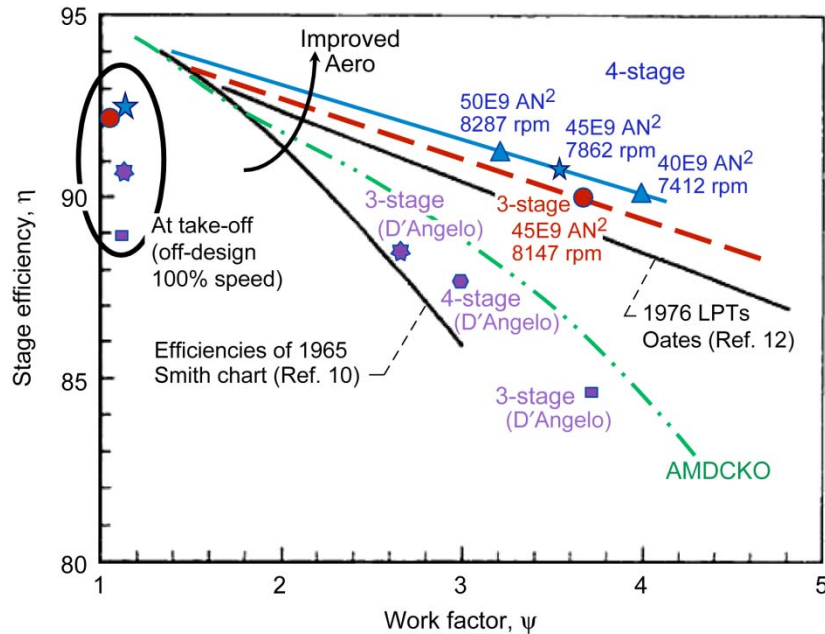


Figure 3.—Turbine design-point stage efficiency versus work factor ( $\Delta h_0/U^2$ ), showing data from Smith (Ref. 10), 1976 LPTs compiled by Oates (Ref. 12), VSPT conceptual designs by D'Angelo (Ref. 5), VSPT conceptual designs for LCTR, and AMDCKO meanline results. Select off-design (100%-speed) efficiencies are shown for reference in the oval.

## Incidence-Tolerant Blade Rows

As a result of the near 50% change in speed, the rotors and embedded stators (nozzles and exit guide vane row) of the variable-speed power turbine will be subject to large (*e.g.*, 40 to 80 degrees, see D'Angelo (Ref. 5)) incidence swings. The calculated incidence variations for LCTR VSPT conceptual designs are documented later in the paper; however, it is instructive to use rudimentary meanline analysis for a single-stage turbine (nozzle/rotor) to quantify the expected influence of the speed variation on the velocity triangles, and their implications regarding variable geometry and incidence levels into embedded blades and vanes.

As described in the previous section, to maintain constant enthalpy extraction while reducing rotor speed from 100% to 50% (for example), a 3.5 to 4-fold increase in work factor is required. There are a number of ways the turbine can achieve the required enthalpy extraction level at the high and low speeds. Using an incompressible analysis, two cases, considered relevant to the LCTR VSPT problem, are considered here:

Case I—Variable geometry and fixed flow ( $u_x$ )

Case II—Fixed geometry and variable flow

Case I represents an attempt to assess requirements for a turbine with variable geometry, while Case II represents a turbine with fixed geometry. The effect of speed factor,  $f = N/N_{100\%}$ , on work factors, flow coefficients, and flow

angles for the two cases is summarized in Table 2 and rotor velocity triangles for the two cases are provided in Figure 4. The associated impact on blade row incidence levels are discussed in the following sub-sections.

### Case I—Variable Geometry and Constant Flow

The use of variable geometry in turbines has traditionally been restricted to variable nozzles used to manage incidence so as to trim for efficiency (see recent study by Chen (Ref. 13)) and to throttle the gas generator (see Rogo and Benstein (Ref. 14) and Karstensen and Wiggins (Ref. 15)). This is accomplished using actuated vanes with variable setting angles, where their complexity and weight are warranted by the efficiency benefit derived. (Variable rotors were deemed technologically inadvisable and outside of the scope of the present effort.) For Case I, the vanes are reset to establish the work factor required to meet the constant  $\Delta h_0$  while maintaining constant axial velocity (mass flow rate). In an engine, the corresponding requirement would be to hold  $\Delta h_0$  while maintaining constant Mach number into the nozzle (in which case the flow coefficient will scale with inverse corrected, rather than physical, speed). To retain constant specific power at a constant mass flow rate, the nozzle needs to be relatively closed at the lower speed to impart increased pre-swirl into the rotor. The changes in  $\alpha_1$ ,  $\beta_1$ , and  $\alpha_2$  associated with difference in VSPT speed at take-off and cruise are provided in Figure 5.

TABLE 2.—EFFECT OF CRUISE-TO-TAKE-OFF SPEED RATIO ( $F$ ) ON WORK FACTORS, FLOW COEFFICIENTS, AND FLOW ANGLES

Cases	$\frac{\psi}{\psi_{100\%}}$	$\frac{\phi}{\phi_{100\%}}$	$\Delta \tan \alpha_1$	$\Delta \tan \beta_1$	$\Delta \tan \alpha_2$
I. Variable geometry and fixed flow	$\frac{1}{f^2}$	$\frac{1}{f}$	$\frac{\psi_{100\%} - f}{\phi_{100\%}}$	$\frac{1-f}{f} \left( \frac{\psi}{\phi} \right)_{100\%}$	$-\frac{1-f}{\phi_{100\%}}$
II. Variable flow and fixed geometry	$\frac{1}{f^2}$	$\frac{1+\psi}{1+\psi_{100\%}}$	0	$\frac{1}{\phi_{100\%}} \left( \frac{\psi - \psi_{100\%}}{1+\psi} \right)$	$\frac{-1}{\phi_{100\%}} \left( \frac{\psi - \psi_{100\%}}{1+\psi} \right)$

Blade row stations 1 = rotor inlet; 2 = rotor exit.

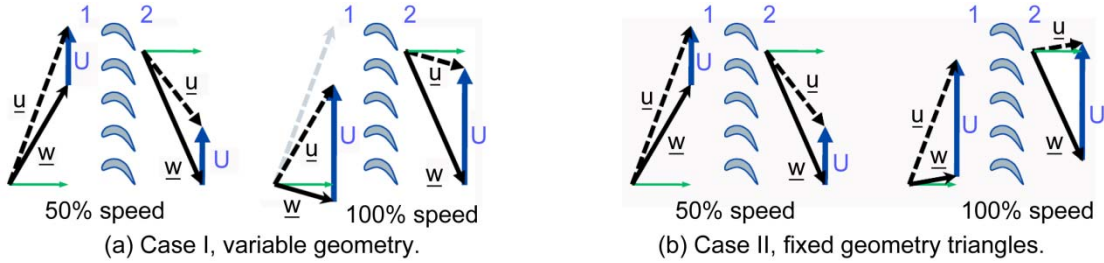


Figure 4.—Rotor velocity triangles (stations 1 and 2) at 50 and 100% VSPT speed.

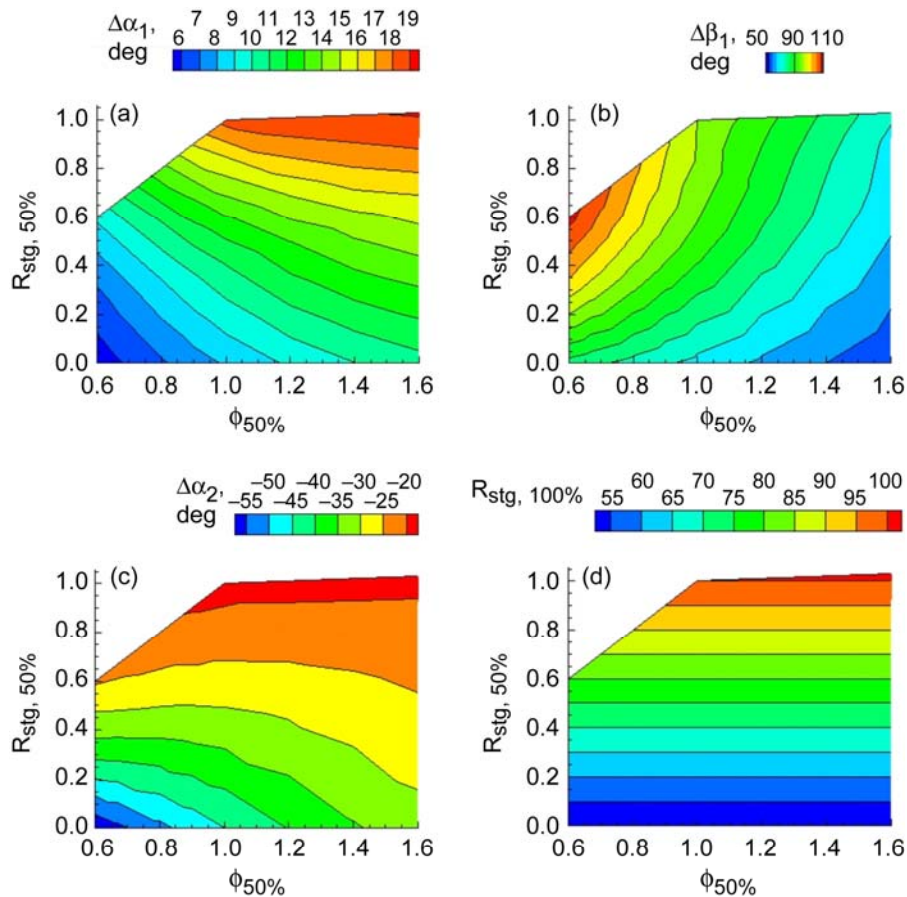


Figure 5.—Results of ADMDKO calculations at  $\psi_{50\%} = 4$  and  $f = 0.5$ , showing (a) variable nozzle reset ( $\Delta \alpha_1$ , deg); (b) change in rotor inlet relative flow angle ( $\Delta \beta_1$ , deg); (c) change in embedded stator/EGV inlet absolute flow angle ( $\Delta \alpha_2$ , deg); and (d) stage reaction at take-off as a function of cruise (50%-speed) flow coefficient and cruise stage reaction.

The flow coefficient at cruise will be set in part by the optimization of overall turbine efficiency at the conceptual design level (see Figs. 2(a) and (b)). For cruise work factors from 3.5 to 4, the flow coefficient will be near unity or greater for optimum efficiency. Considering Figure 5 (and Table 2), for a design of a given stage reaction, the incidence variation for embedded rotors and stators (and exit guide vane) decreases with increasing cruise flow coefficient. In contrast, the nozzle/stator resets increase with increasing cruise flow coefficient. At a given flow coefficient, the nozzle/stator reset requirements and the rotor/stator incidence levels are minimized by setting low stage reactions at cruise. Influenced by this analysis, the stage reaction,  $R_{stg} = 0.3$  was used in the conceptual designs herein. The choice for low stage reaction must be balanced against its deleterious impact on stage efficiency (Fig. 2(c)).

An example Case I stage is shown in Table 3. As shown, to hold  $\Delta h_0$  and  $u_x$  constant, the inlet nozzle would need to be opened by 11-degrees when changing from the cruise design point (54% speed) to take-off (100% speed). In practice, if a variable nozzle were employed, care would need to be taken to insure that reset (closing) of VSPT nozzles/vanes at cruise does reset engine flow (throttle the core, cf. Karstensen and Wiggins (Ref. 15), for example). The nozzle/vane profiles—particularly on the pressure side—may need to be contoured so that sufficient margin on minimum flow area is maintained as vanes are reset.

The change in rotor inlet flow angle is nearly 70 degrees between take-off and cruise (Table 3), representing a substantial incidence swing, and highlighting the need for incidence-tolerant rotors. The Ainley-Mathieson negative ( $i/i_s = -2.7$ ) and positive ( $i/i_s = 1$ ) stall incidence range (Ref. 16) is provided for reference. The change in the absolute

flow angle out of the rotor (or into the downstream embedded stators or exit guide vane) is nearly 35-degrees, with lower swirl angles discharged at take-off speed. This large change in swirl discharged from the rotor highlights the need for incidence-tolerant stator rows in multistage machines, and the likely need for an incidence-tolerant exit-guide-vane (EGV), with associated added-weight, to be installed downstream of the aft-rotor (cf. D'Angelo (Ref. 5)).

### Case II—Fixed Geometry, Variable Flow

Case II is considered an incompressible analog to the engine VSPT with fixed geometry (see LCTR Power Turbine Conceptual Design section). With no variability in the nozzle/stator settings, the axial velocity (flow) must change as shown in Tables 2 and 3 in order to maintain constant specific-power at the various PT speed settings. The flow coefficient is reduced from cruise (50% speed) to take-off (100% speed) by more than 50%. Relative to the variable geometry Case I at  $R_{stg} = 0.3$  (see Table 3), the negative incidence in the rotor is reduced (23-degrees) at take-off (100% speed) while the negative incidence in the downstream stator (or EGV) is increased (23-degrees) at take-off. The rotor reaction for the corresponding 100% design-point (to achieve the same stator and rotor exit flow angles) is only slightly higher (0.42 vs. 0.3) than at the 50% design-point. As seen in Figure 6, the impact of increased stage reaction at a given flow coefficient is to increase rotor incidence variation and to decrease stator incidence variation. A balance is achieved at  $R_{stg} = 0.5$ . The higher stage reaction (relative to  $R_{stg} = 0.3$  of Case I) enhances efficiency as well (see Fig. 2(c)). As found for Case I, the magnitude of incidence variations into the rotor and stator are increased as flow coefficient is reduced at a given work factor (Fig. 6).

TABLE 3.—SINGLE-STAGE TURBINE VELOCITY TRIANGLE CHANGES TO OBTAIN CONSTANT ENTHALPY EXTRACTION WHILE UNDERGOING A 50%-SPEED CHANGE – DESIGNS AT  $M_{r,2} = 0.7$ ,  $Z_r = Z_n = 0.8$

Speed	$\psi$	$\phi$	$\eta_{stg}$	$R_{stg}$	A-M stall incidence, deg.	$\alpha_0$ , deg.	$\alpha_1$ , deg.	$\beta_1$ , deg.	$\beta_2$ , deg.	$\alpha_2$ , deg.
Case I—Constant $\Delta h_0$ and $u_x$ , variable nozzle/stators/EGV										
100%	1	0.6	<sup>b</sup> 96.3	<sup>b</sup> 0.65	<sup>b</sup> +27/-73	0	54.9	-14.0	-62.4	-14.0
<sup>a</sup> 50%	4	1.2	84.4	0.3	+14.1/-38.1	0	66.03	54.8	-62.4	-47.3
Delta	400%	200%	--	--	--	0	+11.2	-68.7	0	-33.3
Case II—Constant $\Delta h_0$ , fixed geometry, variable $u_x$										
100%	1	0.48	<sup>b</sup> 95.7	<sup>b</sup> 0.42	<sup>b</sup> +28.7/-77.4	0	66.0	9.5	-62.4	+9.5
<sup>a</sup> 50%	4	1.2	84.4	0.3	+14.1/-38.1	0	66.0	54.8	-62.4	-47.3
Delta	400%	250%	--	--	--	0	0	-45.8	0	-56.8
100%	1	0.48	<sup>b</sup> 0.959	<sup>b</sup> 0.5	<sup>b</sup> +28.7/-77.4	0	64.4	0.	-64.4	0.
<sup>a</sup> 50%	4	1.2	0.868	0.5	+16.5/-45	0	64.4	51.3	-64.4	-51.3
Delta	400%	250%	--	--	--	0	0	-51.3	0	-51.3
100%	1	0.4	<sup>b</sup> 95.7	<sup>b</sup> 0.5	<sup>b</sup> +28.7/-77.4	0	68.2	0.	-68.2	0.
<sup>a</sup> 50%	4	1.0	0.857	0.5	+14.3/-38.6	0	68.2	56.3	-68.2	-56.3
Delta	400%	250%	--	--	--	0	0	-56.3	0	-56.3

<sup>a</sup>Design point

<sup>b</sup>Value if designed to match  $\alpha_1$  and  $\beta_2$  of cruise design with take-off (100%) work and flow coefficients.

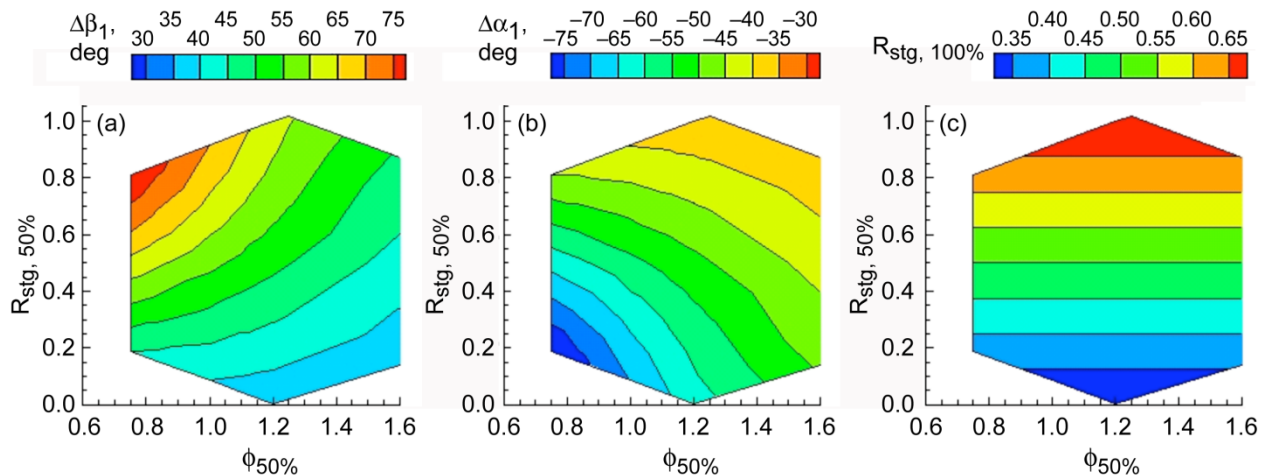


Figure 6.—Results of ADMDKO calculations at  $\psi_{50\%} = 4$  and  $f = 0.5$ , showing (a) change in rotor inlet relative flow angle ( $\Delta\beta_1$ , deg); (b) change embedded stator/EGV inlet absolute flow angle ( $\Delta\alpha_2$ , deg); and (c) stage reaction at takeoff as a function of cruise flow coefficient and cruise (50%-speed) stage reaction.

## Impact of Low Reynolds Number

The 28 kft cruise requirement of the LCTR mission imposes a larger Reynolds number variation (ground to cruise) on the power turbine than encountered in conventional ( $< 15$  kft) rotorcraft operation. The estimated aft-stage unit-Reynolds-numbers (see LCTR Power Turbine Conceptual Design section) are approximately 50,000/in. and 30,000/in. at take-off and cruise altitudes, respectively. The 7500 SHP-class blading is expected to have axial chords of 1 to 2 in., leading to chord Reynolds numbers associated with transitional suction-sides (Haselbach *et al.* (Ref. 17) and Praisner *et al.* (Ref. 18)).

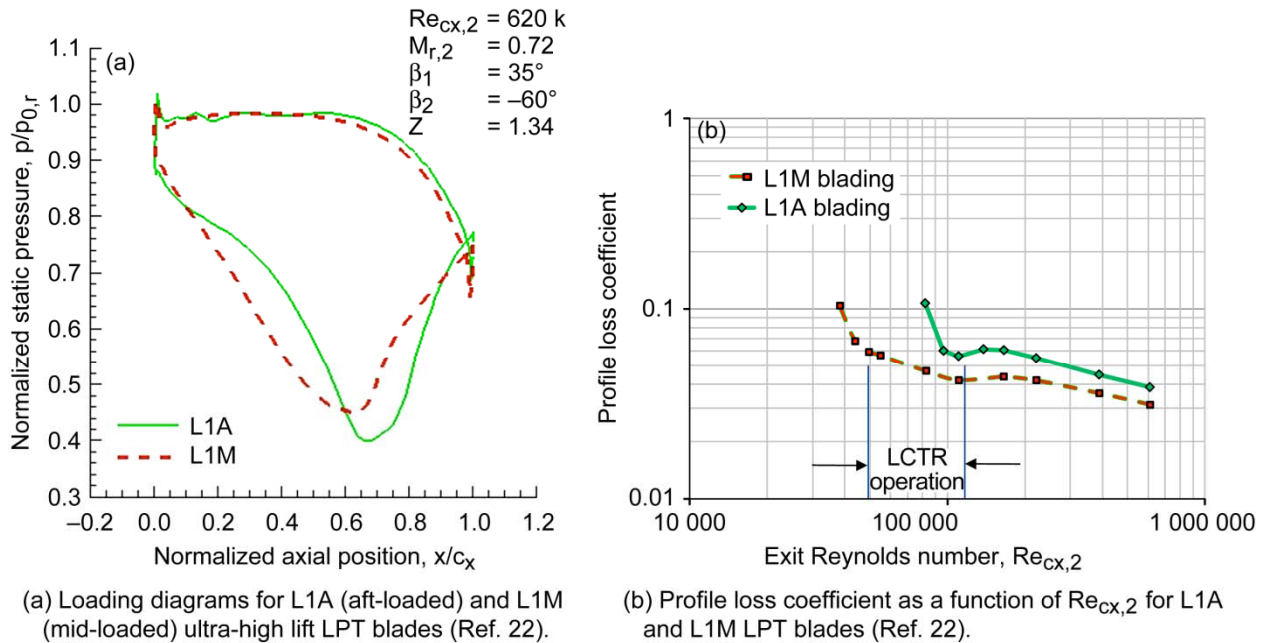
### Design-Point Re Lapse

The loss in design-point performance with altitude due to transitional flow is expected to be analogous to that experienced by larger low pressure turbines (LPT) of modern turbofans (*e.g.*, see Hourmouziadis, (Ref. 19) Haselbach *et al.*, (Ref. 17) and Gier *et al.* (Ref. 20)). The absolute change in Reynolds number will be lower—less variation in pressure from sea-level-static to 28 kft as compared to SLS to 40 kft—but the variation will occur at lower aft-stage chord Reynolds numbers (60 k to 100 k). The need to run at all conditions above the point at which the airfoil stalls, after which loss coefficients rise precipitously, may ultimately set the axial chord of the VSPT blading (see Riegler and Bichlmaier (Ref. 21)). An increase in axial chord, though consistent with reduced blade count, leads to increased length-per-stage and ultimately increased engine length (weight and packaging). Gier *et al.* (Ref. 20) have argued convincingly, counter to recent trends toward ultra-high aerodynamic loading ( $Z > 1.3$ ),

to utilize moderate aerodynamic loading levels ( $0.8 < Z < 1$ ). The optimum loading levels for the LCTR-class turbines are expected to emerge over time as industry, the labs, and academia apply component and engine-level preliminary design/optimization tools to the problem.

The impact of low Reynolds number is firstly a design-point problem, affecting all future turbines of this size class and mission—variable- or fixed-speed. Computed Reynolds number lapse for the Air Force Research Laboratory (AFRL) L1A and L1M high lift blades (Clark *et al.* (Ref. 22)) are provided in Figure 7. The L1-series has Zweifel coefficients at  $Z = 1.34$  and 95-degrees of turning. The blades are considered to be relevant to embedded stages of the LCTR VSPT. The computations were performed using Chima's 2-D Reynolds-Averaged Navier-Stokes (RANS) code (Ref. 23) and Wilcox's low-Re variant of the  $\kappa\text{-}\omega$  model (Ref. 24). The inlet turbulence intensity was set at 5% and the length scale of turbulence was set to achieve the desired freestream turbulent viscosity ( $\mu_t/\mu_l = 0.1$ ). The length scale of turbulence selected strongly affected the location of transition on the suction-side. The C-grids utilized were generated using the GRAPE code (Sorenson (Ref. 25)). The grid spacing was set so that the  $y^+$  near the leading edge at high chord  $Re_{cx,2}$  (620 k) was less than two.

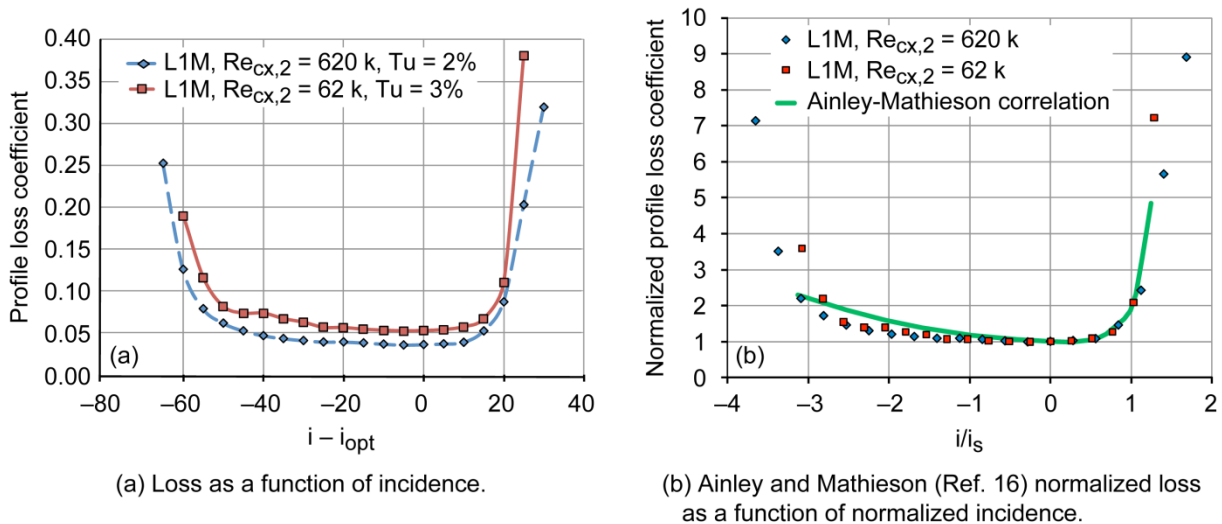
The computed loading diagrams and Reynolds number lapse for the L1A and L1M blade profiles are shown in Figure 7. The blades accomplish the same 95-degrees flow turning, at the same aerodynamic loading level, using mid- and aft-loaded sections (Fig. 7(a)). The loading distribution has an impact on the increase in loss with decreasing chord Reynolds number, though the power-law lapse rates in the fully turbulent ( $Re_{cx,2} > 200$  k) region are similar.



(a) Loading diagrams for L1A (aft-loaded) and L1M (mid-loaded) ultra-high lift LPT blades (Ref. 22).

(b) Profile loss coefficient as a function of  $Re_{cx,2}$  for L1A and L1M LPT blades (Ref. 22).

Figure 7.—Computed loading diagrams and Reynolds lapse rates for aft- (L1A) and mid-loaded (L1M) LPT blading (Clark *et al.*, Ref. 22) accomplishing the same 95-deg flow turning at high aerodynamic loading ( $Z = 1.34$ ).



(a) Loss as a function of incidence.

(b) Ainley and Mathieson (Ref. 16) normalized loss as a function of normalized incidence.

Figure 8.—Computed two-dimensional profile (+ shock) loss coefficients as a function of incidence for L1M blading (Ref. 22) at  $Re_{cx,2} = 620$  k and 62 k and  $M_{r,2} = 0.72$ .

### Impact on Incidence Range

The need for strong incidence-tolerance exacerbates the low-Re challenge. In addition to increased minimum loss, the loss buckets will generally narrow as Reynolds number is reduced. This impact was analyzed using the L1M high lift ( $Z = 1.34$ ) blading. The reduction in incidence range with decreasing  $Re_{cx,2}$  is evident in Figure 8(a). The minimum loss increases with decreasing Reynolds number (increasing altitude, see Fig. 7(b)) and the loss bucket narrows measurably (Fig. 8(a)). The canonical form of the loss bucket (Fig. 8(b)) is

largely retained at the two Reynolds numbers, and is in good agreement with the off-design correlation of Ainley and Mathieson (Ref. 16).

The AMDCKO meanline analysis shows that incidence range decreases, as expected, with increased loading (or reduced axial-chord to pitch ratio for a given turning). In addition to minimizing design-point loss due to Reynolds number lapse, there is a justifiable argument to restrict aerodynamic loading levels ( $Z$ ) to obtain increased incidence range as well.

## LCTR Power Turbine Conceptual Design

As outlined above, key aerodynamic challenges for the VSPT are associated with high work factors at cruise, the need for incident-tolerant blading that can accept rotor inlet flow changes from 40- to 80-degrees and stator/EGV inlet flow angle variations near 30- to 60-degrees, and the lapse in performance and incidence-range associated with the decrease in Reynolds number with altitude. In this section, the aerodynamic requirements are refined via conceptual design of candidate 3- and 4-stage turbines to meet the LCTR engine objectives.

### Design Approach

The designs were carried out using the design- and off-design meanline tools of F. Huber (see Clark *et al.* (Ref. 22)) which are consistent with AMDCKO methodology. The Huber tools are considered to be representative of industry state-of-the-practice in turbine meanline codes. They are used in the present study to set a realistic design space and to generate variables needed for design of detailed blade profiles *vis-à-vis* the AFRL design system (Clark *et al.* (Ref. 22)).<sup>1</sup>

As outlined in the previous sections, the following attributes influenced the design choices of the preliminary conceptual design:

- i.) The LCTR spends a majority of its mission in cruise.
- ii.) The VSPT work factors at cruise are substantially (3.5 to 4 times) higher than at take-off and the associated loss buckets are narrower.
- iii.) The positive-incidence range is substantially (2 to 3 times) narrower than negative-incidence range.
- iv.) The design-point loss increases and the incidence range decreases from take-off to cruise due to Reynolds number lapse.
- v.) The increase in design-point loss due to Re lapse is larger in high lift ( $Z$ ) airfoils than in low lift designs.

The confluence of these multiple factors means that the optimum design-point for the LCTR power turbine will be near the lowest-speed cruise condition (*i.e.*, 54% of take-off speed). The corresponding flow coefficient will likely be near unity or greater, and will be reduced to about half (for 54% speed change) at take-off. The stage reaction at cruise is expected to vary little from that at take-off and should be optimized with consideration of efficiency at cruise and its lapse due to off-design (incidence at take-off). The optimum blade rows are expected to be achieved at moderate aerodynamic loading ( $0.8 < Z < 1$ ).

<sup>1</sup>The author is indebted to Dr. Lisa W. Griffin of NASA Marshall Space Flight Center for permission to use F. Huber's meanline and blade generator codes, developed under earlier SBIR contract, and to Dr. J. P. Clark (AFRL) for use of the AFRL Turbine Design and Analysis System (Ref. 22).

## Setting Speed— $AN^2$ Limited at Take-Off

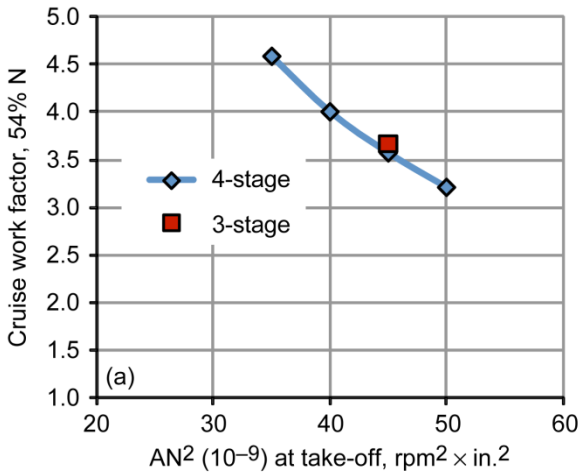
The specific power requirement is set by the engine analysis (see Table 1). In the present study, the cruise and take-off specific power levels are both approximately  $\Delta h_0 = 200$  SHP/lb<sub>m</sub>/s, corresponding to the cruise and take-off pressure ratios shown in Table 1. An average enthalpy extraction per stage is used along with a specified work factor to set the pitchline velocity ( $U^2 = \Delta h_0 / (N_{stg} \psi)$ ). The pitchline velocity sets the product of the pitchline radius and shaft speed. The pitchline radius must be consistent with a rim diameter and the flow area (near 200 to 220 in.<sup>2</sup> in this study, as determined by scaling existing turbine geometries).

The product of the flow area and the square of rpm,  $AN^2$  (rpm<sup>2</sup>·in.<sup>2</sup>), is an indicator of acceptable mechanical stress levels (see Mattingly *et al.* (Ref. 27) and Mattingly (Ref. 28)) based on rim temperatures and material strength and life (creep) properties. The  $AN^2$  mechanical limit is used herein to set the max acceptable VSPT shaft speed. The higher the speed, the lower the required average stage work factor, and generally the higher the design-point turbine efficiency (Figs. 9 and 3).  $AN^2$  varies inversely with work factor as speed is changed ( $AN^2 \sim 1/\psi \sim f^2$ ); therefore, the max-allowable  $AN^2$  must be set at the hotter 100% take-off speed (or contingency power) point, while at cruise the power-turbine operates with low  $AN^2$ . The present study limits take-off  $AN^2$  to the range  $40 \leq AN^2 \leq 50 \times 10^9$  rpm<sup>2</sup>·in.<sup>2</sup>. This high  $AN^2$  range implies that the power turbines operate with lighter weight turbine materials (*e.g.*, Hastelloy) at low rim temperatures (*e.g.*, 1000 °F), predicated on high cooling air requirements, or at higher rim temperature (1300 °F) with heavy and expensive Rene-80 type materials. Rotor taper (0.9 is used for the present study) enables slightly higher  $AN^2$  limits (and see Riegler and Bichlmaier (Ref. 21)).

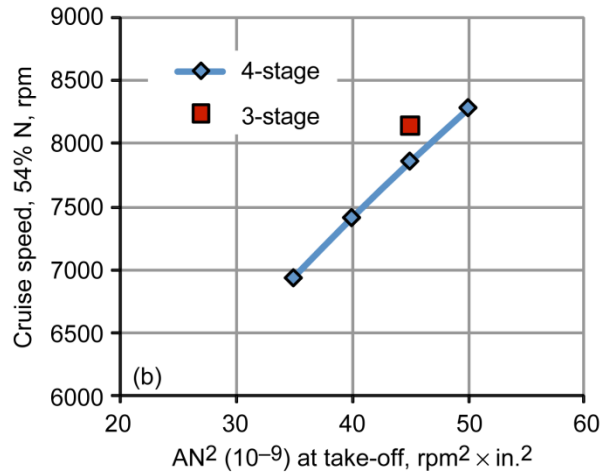
### Conceptual Design Results

Attributes of (preliminary) three- and four-stage  $AN^2$   $45 \times 10^9$  rpm<sup>2</sup>·in.<sup>2</sup> designs are provided in Table 4. The turbines were designed at cruise (54%-speed, 28 kft) with fixed nozzle/stator geometry (Case II above). Corresponding pitchline flow angles are provided in Table 5. The turbine performance was evaluated at the off-design take-off (100% speed, 2 kft) and top-of-climb (100%, 28 kft) flight points, also shown in Table 4. The reported efficiencies predicted by Huber's meanline code (Ref. 22) (see Fig. 3) do not include an exit guide vane, which will likely be required by the level of swirl discharged from the aft-stage rotor at cruise; indeed, D'Angelo (Ref. 5) concluded that a variable EGV might be required.

The design-point efficiencies using the AFRL meanline tool (Ref. 22) were found to be substantially greater than those predicted by the in-house AMDCKO tool (see Fig. 3) and as reported by D'Angelo (Ref. 5) in his study ( $50 \times 10^9$  rpm<sup>2</sup>·in.<sup>2</sup>  $AN^2$  3- and 4-stage designs with EGV, Fig. 3). The



(a) Average work factor as a function of max AN<sup>2</sup>.



(b) VSPT speed at 54% cruise point as a function of max AN<sup>2</sup>.

Figure 9.—Influence of the AN<sup>2</sup> mechanical stress level indicator at take-off on (a) cruise work factor and (b) VSPT speed at cruise.

TABLE 4.—THREE- AND FOUR-STAGE DESIGNS FOR PT REQUIREMENTS OF TABLE 1 (AN<sup>2</sup> = 45×10<sup>9</sup>, Z<sub>n</sub> = 0.8, Z<sub>r</sub> = 1)

	3-stage		4-stage		
	100%	54%	100%	100%	54%
Speed (N/N <sub>100%</sub> )	100%	54%	100%	100%	54%
Altitude	2,000 ft	28,000 ft	2,000 ft	28,000 ft	28,000 ft
VSPT efficiency	0.9212	0.8979	0.9245	0.9222	0.9081
Total-pressure ratio	3.93	5.338	4.00	5.568	5.336
N, rpm	15087	8146	14560	14560	7862
Average $\psi$	1.07	3.67	1.04	1.04	3.57
Average $\phi$	0.49	1.15	0.48	0.48	0.985
Average R <sub>stg</sub>	0.36	0.39	0.41	0.43	0.34
Spool U/V <sub>J</sub>	1.203	0.347	0.781	0.753	0.414
Rotor incidence, deg. (R1, R2, ..., R <sub>Nstg</sub> )	-35.2, -42.8, -54.1	0	-35.5, -41.3, -50.5, -49.0	-44.8, -50.1, -51.0, -39.4	0
Stator incidence, deg (S2, S3, ..., EGV)	-39.0, -49.8, -38.6	0	-43.6, -53.4, -53.8, -36.35	-54.0, -59.1, -49.5, -23.65	0
Power, SHP	5070	2654	5151	2832	2683
Blade count (S/R/Total)	274/304/578		309/340/649		

Design-point

TABLE 5.—DESIGN-POINT FLOW ANGLES AND LOADING FOR 3-STAGE AND 4-STAGE ROTORS (AN<sup>2</sup> = 45×10<sup>9</sup>) AND ULTRA-HIGH LOADING L1-SERIES BLADING (CLARK *et al.* (Ref. 22))

Zweifel	3-stage			4-stage			L1M <sup>a</sup>			L1A <sup>a</sup>		
	1.0	1.0	1.0	1.0	1.0	1.0	1.34	1.34	1.34	1.34	1.34	
Rotor	$\beta_1$	$\beta_2$	Turn	$\beta_1$	$\beta_2$	Turn	$\beta_1$	$\beta_2$	Turn	$\beta_1$	$\beta_2$	Turn
1	55	-65	120	53	-67	120	35	-60	95	35	-60	95
2	50	-58	108	56	-66	122						
3	29	-42	70	46	-57	102						
4	--	--	--	28	-39	66						
h/c <sub>x</sub> R1	2.54			2.36								
h/c <sub>x</sub> R <sub>Nstg</sub>	3.77			4.01								

<sup>a</sup>AFRL ultra-high-load blade shapes provided by Dr. J. P. Clark (AFRL).

performance values are in line with 1976 LPT designs documented by Oates (Ref. 12) (Fig. 3). Nonetheless, a degree of caution is deemed warranted by the calculated high efficiencies at work factors of 3.5 to 4, particularly given the low chord Reynolds numbers. The impact of low-Re efficiency lapse may not be captured fully by the meanline tool, an inference which is supported by the small difference in efficiencies (Table 4) of the 4-stage turbine operating at the two 100% speeds at the substantially different 2-kft and 28-kft Reynolds numbers.

The off-design (100% speed) performance levels (Table 4 and Fig. 3) are worthy of note. Firstly, as shown earlier, the average work factors are low (near unity) due to the increased rotor speed and substantially reduced work factor. The turbine is operating with substantial (30 to 60 degrees) of negative incidence in both rotor and stator rows (Table 4). Nonetheless, the performance levels at this off-design point are predicted to be higher than at the more highly loaded design point. While consistent with the efficiency potential at these low work factors (*e.g.*, 95 to 96% stage efficiency), and with the D'Angelo's (Ref. 5) off-design predictions (Fig. 3), a degree of caution is again warranted.<sup>11</sup>

For completeness, it is noted that it was difficult to achieve a 3-stage design at the  $45 \times 10^9 \text{ rpm}^2 \cdot \text{in.}^2 \text{ AN}^2$  limit. The design was achieved by pushing the engine out in radius (relative to the 4 stage) by a scale factor (1.1) and reducing the annulus flow area—that is, higher N and pitchline speed at the same  $\text{AN}^2$ . Three-stage designs at  $\text{AN}^2$  less than  $45 \times 10^9 \text{ rpm}^2 \cdot \text{in.}^2$  were not achieved. Additionally, Huber's off-design code did not converge on the 100% speed point at 28 kft with the 3-stage. These two findings are taken to be indicative of an aerodynamically marginal 3-stage design. The 4-stage designs were substantially more robust in terms of attaining the design point at various  $\text{AN}^2$  and running at the off-design points.

## VSPT Research Needs

The variable-speed power turbine requirements evidently pose component and blade-row level aerodynamic challenges related to high work factor and loading, required incidence range, and efficiency and incidence-range degradation at low-Re conditions. These challenges lead to research objectives and needs identified in this section.

## High-Load Aerodynamics

The design-approach taken in this effort was to set optimum incidence at the 54% speed, low-Re cruise point, and accept the high (35 to 60-degrees) negative incidence at 100% speed. The design-point challenge is then related to an optimization of performance and weight within mechanical constraints set at take-off (or contingency) power settings. This is a design-

<sup>11</sup> The details of the off-design tool were not available to the author; this cautionary note is not intended as commentary on the accuracy of the meanline tool.

point optimization for which the industry is preeminently qualified. Attainment of maximum efficiencies is expected to require 3-D blading with lean and bow (see, for example, Hourmouziadis (Ref. 19) and Riegler and Bichlmaier (Ref. 21)) and endwall contouring (see, for example, Hartland *et al.*, (Ref. 28) Praisner *et al.*, (Ref. 29) Germain *et al.*, (Ref. 30) and Knezevici *et al.* (Ref. 31)) in order to control secondary-flow and endwall loss production. Thus, there is an identified need to apply advanced design/optimization tools to achieve optimized cruise-point designs. In the context of the variable-speed power turbine, the aerodynamic design-point optimizations may need to be extended to include operation at multiple flight points; further, attainment of high design-point efficiency and incidence range will need to be traded for cost of weight and parts count. Setting the optimum aerodynamic loading level (Z) in the VSPT blade rows will involve consideration of both component and system level impacts.

## Aerodynamics of High Negative Incidence

Arguably the hardest point for the turbine (designed at the 54% speed low-Re cruise point) to achieve is 100% speed at 28 kft altitude (see Table 1). The negative incidence levels at this operating point—as high as 60-degrees in some rows—exceed levels at take-off (100% speed, 2 kft, see Table 4); unfortunately, this occurs at cruise altitude where reduction in range-of-acceptable-loss (Fig. 8) associated with Reynolds number lapse would be most severe. As mentioned, this was the point at which the 3-stage conceptual-design turbine could not operate. The negative 60-degree incidence is only marginally within the predicted pressure-side stall range of Ainley-Mathieson (Ref. 16) ( $i/i_s = -2.7$ ) for a work factor unity stage. There is an identified need to develop blading that mitigates loss associated with strong negative incidence.

A study by Brear *et al.* (Refs. 32 and 33) has showed a 0.6 point efficiency decrement per 10-degrees negative incidence at exit Reynolds numbers of 130 k. The incidence loss was attributed to a separation occurring in the cove region of the blade due to the adverse pressure gradient. Brear *et al.* (Ref. 32) noted that the loss associated negative incidence could be controlled, to some extent, by tailoring the adverse pressure gradient through airfoil pressure-side profiling.

Irrespective of profiling, the loss level at 60-degrees of negative incidence at  $\text{Re}_{c,x,2} = 62\text{k}$  (Fig. 8(a)) is likely unacceptably high. Considering Figure 8(a), 10-degrees of positive incidence could have been accepted at the design point with little impact on loss at cruise (54% speed). This would have reduced the negative incidence requirement at 100% speed, 28 kft point to negative 50-degrees, a point with acceptable loss levels (Fig. 8(a)). This approach would lead to design at somewhat higher speed fraction than required at cruise, though still strongly biased toward minimum speed due to the asymmetry of positive and negative incidence losses (Fig. 8(b)), and the increase in 3-D losses with positive incidence at high aerodynamic loads. In this case, some efficiency at 54% speed (cruise) would be traded for a

reduction in negative incidence (loss) at 100% speed. A key conceptual-design level decision—selection of the speed ratio ( $N_{des}/N_{100\%}$ ) at which to design the VSPT—will determine the balance between positive and negative incidence. To this end, there is an identified need to quantify accurately the 2-D and 3-D loss mechanisms at both high negative incidence and moderate positive incidence.

## **Aerodynamics of Low Reynolds Number Flows**

A key challenge for the 7500 SHP-class power turbine operation at 28 kft is the impact of low Reynolds number on design and off-design performance. Research needs in this area are outlined in this section.

### ***Reynolds Lapse in Meanline Tools***

The meanline tools used in the conceptual design phase need to capture the impact of low Reynolds number on profile and secondary flow loss levels, for both on- and off-design operation. There is an identified need to validate/calibrate the on- and off-design meanline tools to ensure correct prediction of lapse of efficiency and incidence range with altitude.

### ***Sub-Models for Transitional Flow***

Computational tools required for the turbine design, analysis, and optimization—including 2-D and 3-D RANS and unsteady RANS (URANS) solvers and associated turbulence models—require validated sub-models for transitional flow fields. The state of modeling transitional flow fields in turbines was documented by Praisner and Clark (Ref. 34) and Praisner *et al.* (Ref. 18). Their study highlighted the failure of a number of empirical models in the open literature to predict attached and separated-flow transition to the accuracy required for turbine design. Praisner and Clark (Ref. 34) developed transition sub-models and simulation approaches to be used within the  $\kappa$ - $\omega$  model (Ref. 24) that have delivered the required level of accuracy. Their approach represents the state-of-the-art for turbine RANS/URANS flow modeling, and its implementation is being pursued for use during future VSPT turbine blade design efforts.

### ***Impact of Unsteadiness***

Haselbach *et al.* (Ref. 17) and others have highlighted the impact of unsteadiness of wakes from upstream blade rows on the design-point loss levels. The interaction of a passing wake with a laminar/transitional-boundary-layer has been studied in great detail (see, for example, Halstead *et al.* (Ref. 35)). At a given aerodynamic loading level, the loss levels in steady flows were found to be substantially (*e.g.*, 20%) higher than when subjected to wake passing; further, the loss increase with Reynolds number lapse (sensitivity) is mitigated to some degree (see Haselbach *et al.* (Ref. 17)). The aerodynamic loading levels ( $Z$ ) will influence unsteady wake effects by setting effective inlet turbulence intensities, reduced

frequencies, and length scales (cf. Haselbach *et al.* (Ref. 17) and Gier *et al.* (Ref. 20)). There is an identified need to simulate accurately the impact of unsteadiness on the transitional flow fields of the VSPT blade rows.

### ***Impact on Incidence***

The useful range of incidence decreases as Reynolds number lapses with increased altitude (see Fig. 8a). There is an identified need to quantify the effect of Reynolds number on the useful incidence range.

### ***Impact of Aerodynamic Loading Distribution***

The computational results shown earlier (Fig. 7(b)) indicate the potential role of loading distribution in setting loss level, and more subtly lapse rate, at a given Reynolds number. The loading distribution is also expected to play a strong role in setting the useful incidence range of the blade row. In addition to the chordwise loading distribution, the importance of 3-D aerodynamics in controlling secondary flow and endwall losses at off-design conditions (incidence) was reported by Gier *et al.* (Ref. 20) There is an identified need to understand the characteristics of loading schedules that mitigate lapse in efficiency and incidence-range as Reynolds number is reduced.

## **Research Steps at NASA**

Under the NASA Fundamental Aeronautics Program, Subsonic Rotary Wing project, an effort is underway at Glenn Research Center (GRC) to conduct research to enable future variable-speed power turbines for LCTR-class engines. The stepwise approach adopted by the VSPT team is outlined below.

### **VSPT Requirements and Conceptual Design**

A conceptual design of a VSPT that meets the LCTR mission/engine requirements is to be executed and refined to a level that establishes representative vane, blade, and EGV blade flow angle requirements. The performance levels predicted in on- and off-design meanline analyses (Ref. 22) will be used to refine the engine and VSPT requirements.

### **Detailed Design of Incidence-Tolerant Blading**

Incidence-tolerant rotor, vane, and EGV blade shapes that meet the identified VSPT requirements are to be developed using flow angles from the meanline analyses. The envisaged approach utilizes the turbine airfoil design and optimization system developed by Clark *et al.* (Ref. 22) The process includes meanline analyses, through 2-D blade-profile design/optimization and 3-D blade generation (stacking), through 3-D RANS (with mixing-plane) and multi-blade-row URANS calculations (see Clark *et al.* (Ref. 22)).

## Transition Sub-Model Assessment/Implementation

Influenced by the work of Praisner and Clark (Ref. 34), there is an effort underway to assess, and to implement in internal research codes, transition sub-models which are compatible with Wilcox's low-Re  $\kappa$ - $\omega$  turbulence model (Ref. 24). The intent is to develop a validated 3-D RANS/URANS-based computational methodology for simulation of the low-Re flow in multistage VSPT blade rows at on- and off-design (high incidence) conditions. The computational results will be used to refine engine and system level analyses.

## Transonic Cascade Testing of 2-D Sections

Two-dimensional sections of the 3-D VSPT incidence-tolerant rotor/stator/EGV blading are to be tested in NASA GRC transonic linear cascade (Fig. 10). LCTR-relevant exit relative Mach (0.6 to 1+) and unit exit isentropic Reynolds numbers (60 k/in. to 333 k/in.) can be established, and incidence can be varied by 45-degrees. The cascade, described in detail by Giel *et al.* (Ref. 36), is highly three-dimensional and has been used previously to assess heat transfer in blades with transitional flow (Ref. 36); indeed, data from previous entries are being used currently to assess the applicability of the existing turbulence/transition models available in in-house codes. (Note that the minimum Reynolds number attainable at  $M_2 = 0.7$  is just above sea-level take-off conditions, and nearly twice that of cruise conditions; thus, data obtained at flight Reynolds numbers will be at low  $M_2$ .)

## Rotordynamics

Assessment of the mechanical challenges associated with operation of a variable-speed power turbine, although beyond the scope of the present paper, is considered a key part of the VSPT research and technology development effort. Of particular interest are potential constraints imposed on the aerodynamic design by mechanical issues associated with variable speed—for example, torque capacity requirements and operational speeds relative to shaft critical speeds (rotordynamics). To this end, a preliminary design of the LCTR power-turbine shaft is underway, with the intent that any aero-relevant interactions between the shaft and turbine-aero designs be identified.

## VSPT Component Experiment

Initial aero-experiments with developed incidence-tolerant blading will be restricted to the cascade. The experiments will provide valuable data, over a range of Reynolds number and incidence, to be used to validate and calibrate in-house design and analysis tools. In order to include the effects of blade-row interaction, rotation, and leakage flows, plans are to conduct

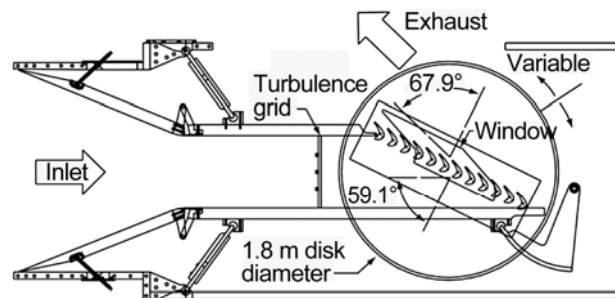


Figure 10.—Schematic diagram of NASA GRC transonic linear cascade (from Giel *et al.*, Ref. 36).

subsequent experiments at the multi-blade-row component level—minimum 1.5 stage (nozzle, rotor, EGV). An assessment of potential in-house and external vehicles for component level VSPT experimentation is currently underway. The assessment includes investigating the viability of utilizing an existing T700-700 test stand to conduct component level research.

## Conclusions

The key aerodynamic challenges of the variable-speed power turbine are related to attainment of efficiency at high work factors (3.5 to 4 at cruise), the wide incidence variation associated with the speed change from take-off (100% speed) to cruise (54% speed), and operation at low chord Reynolds numbers encountered at 28 kft cruise. The efficiency at high work factor will require 3-D blading that manages 2-D (profile and shock losses) and 3-D secondary flow and endwall flow losses. Wake passing (unsteadiness) impacts blade row loss levels of the low-Re flow fields significantly and, therefore, must be accounted for in the design process. The high efficiency blading must also be incidence-tolerant, able to accept changes in incidence angle up to 60-degrees at the most challenging off-design point (100% speed, 28 kft), where particular attention to loss production at high negative incidence will be needed.

The lapse in Reynolds number from sea-level to 28 kft has deleterious impact on both design-point and off-design efficiency levels, and incidence range. The design-point cruise-efficiency at low chord Reynolds number is a technical challenge shared by both fixed- or variable-speed power turbines for the LCTR missions. The high cruise-work-factors and incidence-range requirements of the VSPT exacerbate the Re-lapse issues.

The design of low-loss, incidence-tolerant vane, blade, and EGV blading is considered a key technical challenge for the variable-speed power turbine. At the conceptual-design level, weight ( $AN^2$ , stage count, and blade count) will need to be traded against VSPT efficiency and incidence range. At the blade-row level, reduction of work factors and aerodynamic loading levels ( $Z$ ), tailoring of blade loading schedules, and design/optimization of 3-D blade and endwall profiling, will

aid in attainment of blade rows with required incidence range at satisfactory loss levels. The intent of the VSPT research effort underway at NASA GRC is to develop experimentally validated design methods and computational tools required for the design and optimization of incidence-tolerant blade rows for the variable-speed power turbines of the LCTR application.

## References

- Johnson, W., Yamauchi, G.K., and Watts, M.E., "NASA Heavy Lift Rotorcraft Systems Investigation," NASA TP-2005-213467, Sep., 2005.
- Wilkerson, J.B. and Smith, R.L., "Aircraft System Analysis of Technology Benefits to Civil Transport Rotorcraft," NASA/CR-2009-214594, June, 2009.
- Acree, C.W., Hyeonsoo, Y., and Sinsay, J.D., "Performance Optimization of the NASA Large Civil Tiltrotor," *Proc. Int. Powered Lift Conf.*, London, UK, July 22–24, 2008.
- Acree, C.W., Jr., "Integration of Rotor Aerodynamic Optimization With the Conceptual Design of a Large Civil Tiltrotor," *Proc. AHS Aeromechanics Conf.*, San Francisco, Jan. 2010.
- D'Angelo, M., "Wide Speed Range Turboshaft Study," NASA CR-198380, August 1995.
- Snyder, C.A. and Thurman, D.R., "Gas Turbine Characteristics for a Large Civil Tilt-Rotor (LCTR)," *Proc. AHS Int. 65th Ann. Forum*, TX, May, 2009.
- Ainley, D.G. and Mathieson, G.C.R., "A Method of Performance Estimation for Axial-Flow Turbines," Aeronautical Research Council (ARC), R&M 2974, 1957.
- Dunham, J. and Came, P.M., "Improvements to the Ainley-Mathieson Method of Turbine Performance Prediction," *J. Eng. for Power*, July, 1970, pp. 252–256.
- Kacker S.C., and Okapuu. U., "A Mean Line Prediction Method for Axial Flow Turbine Efficiency," *J. Eng. Power*, 104, Jan, 1982, pp. 111–119.
- Smith, S.F., "A Simple Correlation of Turbine Efficiency," *J. Royal Aero. Soc.*, 69, 1965, pp. 467–470.
- Horlock, J.H., *Axial Flow Turbines*, Krieger Publishing Co., USA, 1985, p. 127.
- Oates, G.C, *Aerothermodynamics of Aircraft Engine Components*, AIAA Education Series, 1985.
- Chen, S-C, S., "Preliminary Axial Flow Turbine Design and Off-design Performance Analysis Methods for Rotary Wing Aircraft Engines; II-Applications," *Proc. AHS Inter. 65th Ann. Forum*, TX, May, 2009.
- Rogo, C. and Benstein, E.H., "Variable Cycle Turboshaft Technology for Rotorcraft of the '90s," *J. Propulsion*, 2 (1), Jan-Feb, 1986, pp. 73–80.
- Karstensen, K.W. and Wiggins, J.O., "A Variable-Geometry Power Turbine for Marine Gas Turbines," *J. Turbomachinery*, 112, Apr 1990, pp. 165–174.
- Ainley, D.G. and Mathieson, G.C.R., "An Examination of Flow and Pressure Losses in Blade Rows of Axial Turbines, British Aeronautical Research Council (ARC)," R&M 2891, 1955.
- Haselbach, F., Schiffer, H.-P., Horsman, M., Dressen, S., Harvey, N., and Read, S., "The Application of Ultra High Lift Blading in the BR715 LP Turbine," *J. Turbomachinery*, 124, Jan 2002, pp. 45–51.
- Praisner, T.J., Grover, E.A., Rice, M.J., and Clark, J.P., "Predicting Transition in Turbomachinery – Part II: Model Validation and Benchmarking," *J. Turbomachinery*, 129, Jan, 2007, pp. 14–22.
- Hourmouziadis, J., "Aerodynamic Design of Low Pressure Turbines," in *Blading Design for Axial Turbomachines*, AGARD-LS-167, pp. 8-1 to 8-40, 1989.
- Gier, J., Franke, M., Hübner, N. and Shröder, T., "Designing LP Turbines for Optimized Airfoil Lift," ASME-GT2008-51101, 2008.
- Riegler, C. and Bichlmaier, C., "The Geared Turbofan Technology – Opportunities, Challenges and Readiness Status," *Proc. 1st CEAS European Air and Space Conf.*, Sept. 2007.
- Clark, J.P., Koch, P.J., Ooten, M.K., Johnson, J.J., Dagg, J., McQuilling, M.W., Huber, F. and Johnson, P.D., "Design of Turbine Components to Answer Research Questions in Unsteady Aerodynamics and Heat Transfer," AFRL-RZ-WP-TR-2009-2180, (Internal Report) Sept. 2009.
- Chima, R.V., "Explicit Multigrid Algorithm for Quasi-Three-Dimensional Viscous Flows in Turbo-machinery," *J. Propulsion and Power*, 3 (5), Sept-Oct, 1987, pp. 397–405.
- Wilcox, D.C., *Turbulence Modeling for CFD*, DCW Industries, Inc. La Canada, CA, 1994.
- Sorenson, R.L., "A Computer Program to Generate Two-Dimensional Grids About Airfoils and Other Shapes by Use of Poisson's Equation," NASA TM-81198, 1980.
- Mattingly, J.D., Heiser, W.H., and Daley, D.H., *Aircraft Engine Design*, American Institute of Aeronautics and Astronautics, Wash., D.C., 1987, pp. 562–574.
- Mattingly, J.D., *Elements of Gas turbine Propulsion*, McGraw-Hill, Inc., NY, 1996, pp. 926–929.
- Hartland, J.C., Gregory-Smith, D. G., Harvey, N. W., Rose, M.G., "Nonaxisymmetric Turbine End Wall Design: Part II – Experimental Validation," *J. Turbomachinery*, 122, Apr, 2000, pp. 286–293.
- Praisner, T.J., Allen-Bradley, E., Grover, E.A., Knezevici, D.C., and Sjolander, S.A., "Application of Non-Axisymmetric Endwall Contouring to Conventional and High-Lift Turbine Airfoils," ASME GT2007-27579, 2007.
- Germain, T., Nagel, M., Raab, M., Schüpbach, P., Abhari, R.S., Rose, M., "Improving Efficiency of a High Work Turbine Using Nonaxisymmetric Endwalls – Part I: Endall Design and Performance," *J. Turbomachinery*, 132, Apr, 2010, pp. 021007-1 to -9.

31. Knezevici, D.C., Sjolander, S.A., Praisner, T.J., AllenBradley, E., Grover, E.A., "Measurements of Secondary Losses in a Turbine Cascade With the Implementation of Nonaxisymmetric Endwall Contouring," *J. Turbomachinery*, 132, Jan, 2010, pp. 011013-1 to -10.
32. Brear, M.J., Hodson, H.P., and Harvey, N.W., "Pressure Surface Separations in Low-Pressure Turbines – Part I: Midspan Behavior," *J. Turbomachinery*, 124, July, 2002, pp. 393–401.
33. Brear, M.J., Hodson, H.P., Gonzalez, P., and Harvey, N. W., "Pressure Surface Separations in Low-Pressure Turbines – Part II: Interactions with Secondary Flow," *J. Turbomachinery*, 124, July, 2002, pp. 402–409.
34. Praisner, T.J. and Clark, J.P., "Predicting Transition in Turbomachinery – Part I: A Review and New Model Development," *J. Turbomachinery*, 129, Jan 2007, pp. 1–13.
35. Halstead, D.E., Wisler, D.C., Okishii, T.H., Walker, G.J., Hodson, H.P, Shin, H-W., "Boundary Layer Development in Axial Compressors and Turbines: Part 3 of 4—LP Turbines," *J. Turbomachinery*, 119, 1997, pp. 225.
36. Giel, P.W., Boyle, R.J., and Bunker, R.S., "Measurements and Predictions of Heat Transfer on Rotor Blades in a Transonic Turbine Cascade," *J. Turbomachinery*, 126, Jan, 2004, pp. 110–121.

REPORT DOCUMENTATION PAGE			Form Approved OMB No. 0704-0188	
<p>The public reporting burden for this collection of information is estimated to average 1 hour per response, including the time for reviewing instructions, searching existing data sources, gathering and maintaining the data needed, and completing and reviewing the collection of information. Send comments regarding this burden estimate or any other aspect of this collection of information, including suggestions for reducing this burden, to Department of Defense, Washington Headquarters Services, Directorate for Information Operations and Reports (0704-0188), 1215 Jefferson Davis Highway, Suite 1204, Arlington, VA 22202-4302. Respondents should be aware that notwithstanding any other provision of law, no person shall be subject to any penalty for failing to comply with a collection of information if it does not display a currently valid OMB control number.</p> <p>PLEASE DO NOT RETURN YOUR FORM TO THE ABOVE ADDRESS.</p>				
<b>1. REPORT DATE (DD-MM-YYYY)</b> 01-08-2010		<b>2. REPORT TYPE</b> Technical Memorandum		<b>3. DATES COVERED (From - To)</b>
<b>4. TITLE AND SUBTITLE</b> Assessment of Aerodynamic Challenges of a Variable-Speed Power Turbine for Large Civil Tilt-Rotor Application			<b>5a. CONTRACT NUMBER</b>	
			<b>5b. GRANT NUMBER</b>	
			<b>5c. PROGRAM ELEMENT NUMBER</b>	
<b>6. AUTHOR(S)</b> Welch, Gerard, E.			<b>5d. PROJECT NUMBER</b>	
			<b>5e. TASK NUMBER</b>	
			<b>5f. WORK UNIT NUMBER</b> WBS 877868.02.07.03.01.02.01	
<b>7. PERFORMING ORGANIZATION NAME(S) AND ADDRESS(ES)</b> National Aeronautics and Space Administration John H. Glenn Research Center at Lewis Field Cleveland, Ohio 44135-3191			<b>8. PERFORMING ORGANIZATION REPORT NUMBER</b> E-17334	
<b>9. SPONSORING/MONITORING AGENCY NAME(S) AND ADDRESS(ES)</b> National Aeronautics and Space Administration Washington, DC 20546-0001			<b>10. SPONSORING/MONITOR'S ACRONYM(S)</b> NASA	
			<b>11. SPONSORING/MONITORING REPORT NUMBER</b> NASA/TM-2010-216758	
<b>12. DISTRIBUTION/AVAILABILITY STATEMENT</b> Unclassified-Unlimited Subject Categories: 01, 02, 07, and 09 Available electronically at <a href="http://gltrs.grc.nasa.gov">http://gltrs.grc.nasa.gov</a> This publication is available from the NASA Center for AeroSpace Information, 443-757-5802				
<b>13. SUPPLEMENTARY NOTES</b>				
<b>14. ABSTRACT</b> The main rotors of the NASA Large Civil Tilt-Rotor notional vehicle operate over a wide speed-range (100% at take-off to 54% at cruise). The variable-speed power turbine, when coupled to a fixed-gear-ratio transmission, offers one approach to accomplish this speed variation. The key aero-challenges of the variable-speed power turbine are related to high work factors at cruise, where the power turbine operates at 54% of take-off speed, wide incidence variations into the vane, blade, and exit-guide-vane rows associated with the power-turbine speed change, and the impact of low aft-stage Reynolds number (transitional flow) at 28 kft cruise. Meanline and 2-D Reynolds-Averaged Navier-Stokes analyses are used to characterize the variable-speed power-turbine aerodynamic challenges and to outline a conceptual design approach that accounts for multi-point operation. Identified technical challenges associated with the aerodynamics of high work factor, incidence-tolerant blading, and low Reynolds numbers pose research needs outlined in the paper.				
<b>15. SUBJECT TERMS</b> Simulation; Jet mixing flow; Propellant tanks				
<b>16. SECURITY CLASSIFICATION OF:</b>			<b>17. LIMITATION OF ABSTRACT</b>  UU	<b>18. NUMBER OF PAGES</b> 21
<b>a. REPORT</b> U	<b>b. ABSTRACT</b> U	<b>c. THIS PAGE</b> U		
				<b>19b. TELEPHONE NUMBER (include area code)</b> 443-757-5802



